



ELSEVIER

Available online at www.sciencedirect.com

SCIENCE @ DIRECT®

Physica C 385 (2003) 539–543

PHYSICA C

www.elsevier.com/locate/physc

Current distribution maps in large YBCO melt-textured blocks

M. Carrera ^{a,*}, J. Amorós ^b, A.E. Carrillo ^c, X. Obradors ^{c,*}, J. Fontcuberta ^c

^a *Dep. Medi Ambient i Ciències del Sòl, Universitat de Lleida, Jaume II, 69, 25001 Lleida, Spain*

^b *Dep. Matemàtica Aplicada I, Universitat Politècnica de Catalunya, Diagonal 647, 08028 Barcelona, Spain*

^c *Institut de Ciència de Materials de Barcelona, CSIC, Campus UAB, 08193 Bellaterra, Spain*

Received 30 October 2002; accepted 31 October 2002

Abstract

We report on the progress on computing the current maps from the magnetic induction in bulk samples of YBCO melt-textured compounds. Typical sample size is in the cm range and induction maps $B_z(x, y, z)$ are obtained by Hall probe measurements. Currents are obtained by solving the inverse Biot–Savart problem. No assumption is required on the number of domains or geometry of the sample; the only constraint in the model is that the current circulation should be confined in the basal plane and uniform in the sample thickness. A current map with a resolution of 0.25–0.5 mm is typically obtained. Critical tests of the stability and accuracy of the current flow solutions have been performed. We have applied the algorithms to remanent flux maps obtained after both FC and ZFC magnetization processes. The algorithms can be readily used and thus can constitute a helpful tool for superconductivity engineers. The use of our software implementation is available free of charge at <http://jaumetor.upc.es:8080/caragol>.

© 2002 Elsevier Science B.V. All rights reserved.

Keywords: Bulk YBCO melt-textured; Inverse Biot–Savart problem

1. Introduction

The use of large YBCO melt-textured blocks in practical applications requires a detailed understanding of current patterns. Many previous works have dealt with the inversion problem to obtain current maps from spatially resolved induction measurements. The first relevant works were based in models which assumed cylindrical symmetry for the samples and the current distribution [1–3]. Afterwards, Grant et al. [4] developed a model for square-section thin films based on the discretiza-

tion of the magnetization on a 2-d grid over the sample, while Xing et al. [5], and Kamijo and Kawano [6] used a computation methodology based on the linearization and matrix inversion which was applied to 2-d samples. Keeping the planar approximation to the distribution of current, extensions of the discretization and matrix inversion method were made to 3-d samples by Wijngaarden et al. [7,8], Jooss et al. [9] and Amorós et al. [10]. First, a method was proposed which solves the resulting discrete linear problem by means of Fourier transform [7,9], and later an extension of the method was proposed using fast Fourier transform with a conjugate gradient [8]. Both methods have been applied to obtain current distribution from magneto-optical flux

* Corresponding authors.

E-mail addresses: mcarrera@eup.udl.es (M. Carrera), xavier.obradors@icmab.es (X. Obradors).

imaging experiments. Our method applies QR decomposition by Householder hyperplane reflection to the linear inversion problem, in order to keep at a minimum the propagation of errors arising from the measure of the magnetic field. This procedure has been applied successfully to melt-textured bulk samples [10–12]. Finally, Portabella et al. [13] solved the inversion problem by a finite-element procedure that may be applied to 3-d samples without any regularity assumption, but with important computational requirements.

In the present work we report further analysis of the current distribution computation following the procedure previously proposed [10]. We show that the calculation procedure can be validated in two independent ways: (i) by direct computation of the field B_z induced by our calculated current, and (ii) by computation of the current from measurements of B_z at different heights above the sample. Validation of the computed current is necessary because the homogeneity in the z -axis cannot be assured a priori, and the propagation of experimental errors from the measured B_z to the computed current \mathbf{J} is a very serious problem in bulk samples.

2. Computation method

The algorithm used for the computation of critical currents is described in detail in [10]. Our method assumes two conditions: (i) the current circulation is horizontal (i.e. confined in the basal plane), (ii) there is uniformity in the z -axis, so that the current circulation is the same in all horizontal sections. We do not require any further homogeneity condition on the current circulation within the basal planes. This method is based on the discretization of the magnetization M on the sample: the assumption that M is constant in the cells of a 3-d grid turns the problem of finding its values from the measured B_z into solving a linear system of equations. The main difficulty that we have encountered in the use of this linearization scheme to 3-d bulk samples is the propagation of the experimental error from the experimental B_z measurements to the computed magnetization M [14]. Fast algorithms for the resolution of linear systems may greatly increase the relative error in the calculated M values

as compared to the relative error with which B_z is known. Given the size of the system, this error term would dominate over the actual solution in a bulk sample computation, unless an overdetermined scheme is employed in which one measures B_z at several points for every discrete element of M . Thus, we compute M from overdetermined systems, and, in order to minimize the propagation of the experimental error in B_z we perform the least square resolution by QR decomposition through Householder reflection. This method for the resolution of determined and overdetermined linear systems limits the propagation of error from the independent term to the solution [15]. We keep track of the condition number of the linear system, which measures this propagation. Finally, the current $\mathbf{J}(J_x, J_y)$ is computed as the curl of the discretized M .

We have added to our program the converse computation of the magnetic field $B_z(x, y)$ induced by the computed current at the grid of points of the original measurement, through numerical integration of the Biot–Savart law.

3. Experimental

Single domain melt-textured YBCO samples have been grown by the top seeding method using melt-textured $\text{NdBa}_2\text{Cu}_3\text{O}_7$ seeds and for different starting compositions of the YBCO/Y211 phases [16,17]. This melt-texturing process yields single domain growth up to the borders of the pellet and is oriented with the a – b plane of the crystal parallel to the sample surface. Measurements of the $H\parallel c$ component of remanent magnetic flux maps using a Hall probe technique have been made at 77 K, in which the field was applied with a SmCo (diameter 25 mm, height 20 mm) permanent magnet. This report focuses on results obtained in a sample with nominal composition Y123 + 0.63 Y211 + 0.06 CeO_2 and a cylindrical shape (12 mm diameter, 3 mm thick). An applied field of $\mu_0 H_{\text{ap}} = 0.33$ T was used in this study.

4. Calculated current distribution maps

Fig. 1 shows the trapped field distribution in our sample after a FC process, where the unique

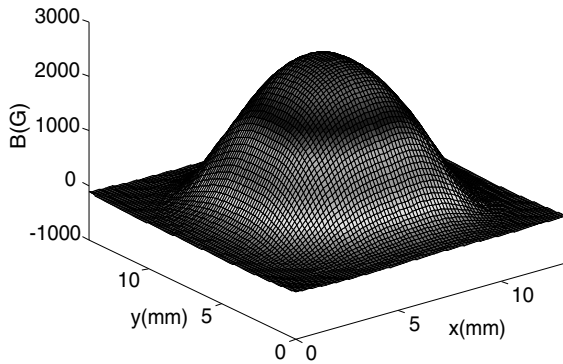


Fig. 1. Remanent flux map measured after a FC process ($z = 0.5$ mm).

central peak ($B \sim 2550$ G) is observed, as expected for a single domain sample. Circulating current vectors calculated from this distribution (Fig. 2) form a regular square-shaped distribution, associated with the X-cross geometry of the growth sectors generated during a top seeding growth process [18]. Critical current density computed in a 0.4×0.4 mm grid is shown in Fig. 3 in three sections along the y -axis for central values of the x -axis. Irregularities are inherent to the differentiation process. In general, however, we observe an approximately constant current density ring of

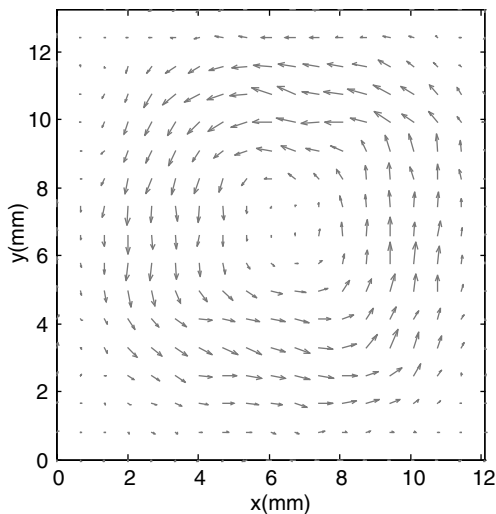


Fig. 2. Circulating current vectors calculated from flux mapping shown in Fig. 1.

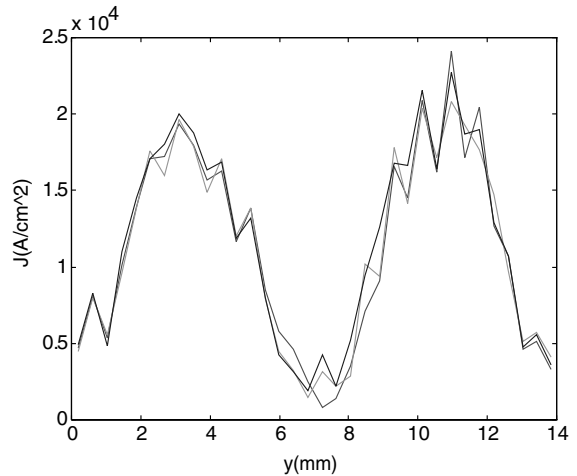


Fig. 3. Current density profiles (absolute value) calculated from flux map of Fig. 1. The three profiles represented in the figure correspond to three sections along the y -axis in the central values of x -axis in the flux map.

1.8×10^4 A/cm², which is in good agreement to that obtained in samples with the same composition by inductive critical current measurements performed with the SQUID magnetometry [16,17].

In a ZFC process the double-peak structure in the remanent flux profile has been found, denoting that full penetration was not achieved, i.e. $H_{ap} < 2H^*$, where H^* is the field at which the flux fronts merge at the sample center. Circulating current computed from this map shows that two current loops of opposite polarity flow around the sample, as expected in this case.

5. Validation of the results

It was not known a priori whether the samples studied fulfilled the conditions of planar circulation and uniformity along the vertical axis that are required by our computation of the critical current. This has been verified with a quantifiable margin of error in two ways: (i) computation of the critical current on the same sample from different sets of measurements of the magnetic field B_z performed at varying heights z above the sample, (ii) comparison of the measured magnetic field B_z with that induced by the computed critical

current. The latter procedure serves as an a posteriori test of whether a given sample fulfills the planar current circulation and symmetry along the z -axis conditions. Both methods of validation of the results have been carried out in the samples studied here, in other measured samples and also in a set of simulations [14].

The vertical magnetic field has been measured in a FC process on grids at heights of 0.5, 0.8 and 1.2 mm, above the sample and all the computations of critical current agree. This agreement would be impossible if the current density and circulation varied significantly from layer to layer within the horizontal layers of the sample. The contribution of every layer to the magnetic field depends on the distance from the given layer to the measurement point, so that the best approximation by the magnetic field generated by a vertically symmetric current would vary with the height above the sample at which we measure B_z . In this case the computed \mathbf{J} would be different at every height.

A clearer verification of our computation of current density is the comparison of the measured magnetic field B_z with that induced by our calculated solution, which may be computed readily by numerical integration of the Biot–Savart law. We have performed this direct computation of the field B_z induced by the computed current for all of our

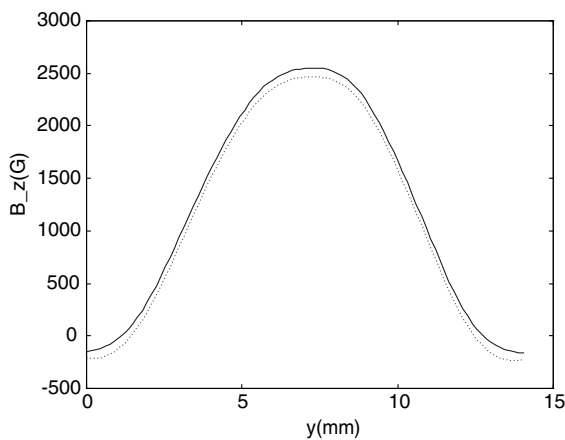


Fig. 4. Measured (continuous line) and calculated (dotted line) B_z profiles for a FC process at $z = 0.5$ mm. The profiles correspond to the sections along the y -axis in the central value of x -axis in the flux map.

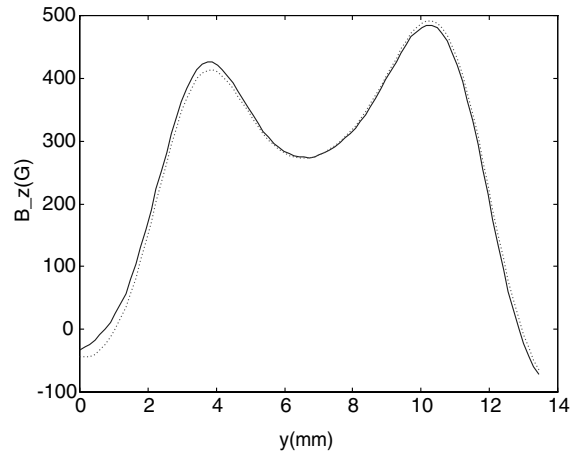


Fig. 5. Measured (continuous line) and calculated (dotted line) B_z profiles for a ZFC process at $z = 0.5$ mm. The profiles correspond to the sections along the y -axis in the central value of x -axis in the flux map (not shown).

measurements and inverse computations. For the FC process with magnetic field B_z measured at $z = 0.5$ mm, Fig. 4 shows the comparison between the experimental and computed magnetic field represented in a section at the central value of x . The absolute difference between the two fields is less than 80 G, and the relative error in the central area is about 2%. For the ZFC process with magnetic field measured at $z = 0.5$ mm (Fig. 5), outside the boundary band where the field vanishes the absolute difference between the two fields is less than 10 G, and the relative error is less than 3%.

6. Conclusions

We have shown that the computation of spatially resolved critical currents in superconducting samples is feasible if we assume horizontal current circulation and uniformity in all planes perpendicular to the vertical magnetic field above the sample. We have used a discretization and least square approximation method which allows to analyze samples at the cm scale with typical spatial resolutions 0.25–0.5 mm. It is possible to check a posteriori whether a given sample fulfills the planarity and vertical uniformity assumptions that we have made and the accuracy of our computation.

No further assumption of homogeneity of the domains or geometry of the sample is required. Our procedure for computing critical currents does not assume homogeneity of planar distribution of current.

The experimental error in the measurement of B_z and its propagation throughout the computation is a critical limiting factor for inverse computation of \mathbf{J} in bulk samples by discretization and matrix inversion. The resolution method for the linear system must take this problem into account.

This computational method has been implemented as the *Caragol* package, which can be used freely to compute critical current circulations through the Internet at the address: <http://jaumator.upc.es:8080/caragol>.

Acknowledgements

This work has been supported by CICYT (MAT99-0855-C02-01) and by Generalitat de Catalunya (1999SGR-206).

This work is dedicated to Professor D. Gonzalez from the University of Zaragoza and ICMA-CSIC on the occasion of his retirement.

References

- [1] D.J. Frankel, J. Appl. Phys. 50 (1979) 5402.
- [2] M. Daümling, D.C. Larbalestier, Phys. Rev. B 40 (1989) 9350.
- [3] L.W. Conner, A.P. Malozemoff, Phys. Rev. B 43 (1991) 402.
- [4] P.D. Grant, M.W. Denhoff, W. Xing, P. Brown, S. Govorkov, J.C. Irwin, B. Heinrich, H. Zhou, A.A. Fife, A.R. Cragg, Physica C 229 (1994) 289.
- [5] W. Xing, B. Heinrich, Z. Hu, A. Fife, A. Cragg, J. Appl. Phys. 76 (1994) 4244.
- [6] H. Kamijo, K. Kawano, IEEE Trans. Appl. Supercond. 7 (1997) 1228.
- [7] R.J. Wijngaarden, H.J.W. Spoelder, R. Surdeanu, R. Griessen, Phys. Rev. B 54 (1996) 6742.
- [8] R.J. Wijngaarden, K. Heeck, H.J.W. Spoelder, R. Surdeanu, R. Griessen, Physica C 295 (1998) 177.
- [9] Ch. Jooss, A. Forkl, R. Warthmann, H. Kronmüller, Physica C 299 (1998) 215.
- [10] J. Amorós, M. Carrera, X. Granados, J. Fontcuberta, X. Obradors, Applied Superconductivity 1997, Inst. Phys. Conf. Series No. 158, 1997, pp. 1639–1642.
- [11] R. Yu, J. Mora, F. Sandiumenge, N. Vilalta, V. Gomis, B. Martínez, E. Rodríguez, J. Amorós, M. Carrera, X. Granados, D. Camacho, J. Fontcuberta, X. Obradors, IEEE Trans. Appl. Supercond. 7 (1997) 1809.
- [12] E. Mendoza, M. Carrera, E. Varesi, A.E. Carrillo, T. Puig, J. Amorós, X. Granados, X. Obradors, Applied Superconductivity 1999, Inst. Phys. Conf. Series No. 167, 2000, p. 127.
- [13] E. Portabella, R. Palka, H. May, W.R. Canders, Applied Superconductivity 1999, Inst. Phys. Conf. Series No. 167, 2000, p. 1063.
- [14] M. Carrera, J. Amorós, X. Obradors, J. Fontcuberta, in press.
- [15] G. Golub, C.F. Van Loan, Matrix computations, second ed., The John Hopkins University Press, 1989.
- [16] X. Obradors, R. Yu, F. Sandiumenge, B. Martínez, N. Vilalta, V. Gomis, T. Puig, S. Piñol, Supercond. Sci. Technol. 10 (1997) 884.
- [17] E. Mendoza, T. Puig, E. Varesi, A.E. Carrillo, J. Plain, X. Obradors, Physica C 334 (2000) 7.
- [18] P. Diko, Supercond. Sci. Technol. 13 (2000) 1202.